Desalination and Water Treatment
www.deswater.com

doi: 10.1080/19443994.2014.911115

55 (2015) 173–182
June

Taylor & Francis
Taylor & Francis Group

Synthesis of magnetic silica with quaternary ammonium salt and its application for chromium(VI) removal

Wei Yao[a], Pinhua Rao[a,*], Yongtao Du[a], Wenqi Zhang[a], Tongzhou Liu[b]

[a]*School of Chemistry and Chemical Engineering, Shanghai University of Engineering Science, Longteng Rd. 333, Songjiang, Shanghai 201620, China, Tel./Fax: +86 21 6779 1214; email: raopinhua@hotmail.com*
[b]*Harbin Institute of Technology Shenzhen Graduate School, Shenzhen 518055, China*

Received 30 September 2013; Accepted 30 March 2014

ABSTRACT

The contamination of water bodies with heavy metals (e.g. chromium and arsenic) is a major problem. Thus, the demand for effective ways of removing these toxic ions is increasing. In this study, a novel quaternary ammonium salt (QAS) was designed and synthesised *in situ* on the surface of silica-encapsulated iron oxide nanoparticles (SEION) to be easily separated by an external magnet. The SEION grafted with QAS (QAS-SEION) were characterised by X-ray diffraction, transmission electron microscopy, Fourier transform infrared spectroscopy, scanning electron microscopy with energy dispersive X-ray spectroscopy and zeta potential. Adsorption experiments were conducted to evaluate the capacity of QAS-SEION for removing Cr(VI) from water. The results indicated that the adsorption of Cr(VI) on the QAS-SEION reached equilibrium within 120 min. A pseudo-second-order model was befitting to describe the kinetics of Cr(VI) adsorption. The adsorption isotherm of Cr(VI) on the QAS-SEION was observed to fit both the Langmuir isotherm equation and Freundlich isotherm equation notably well. The maximum adsorption amount calculated by the Langmuir isotherm equation was close to that obtained by experiment. Overall, QAS-SEION is a promising material for the removal of Cr(VI) from contaminated water.

Keywords: Quaternary ammonium salt; Magnetic silica; Adsorption; Hexavalent chromium

1. Introduction

Water contamination by Cr(VI), primarily existing in the form of anions, has recently become an issue of worldwide concern because Cr(VI) is carcinogenic, mutagenic and teratogenic to living organisms [1]. Cr(VI)-containing wastewater emitted from various industrial operations (e.g. metallurgy and leather tanning) is usually discharged into domestic sewage systems with little treatment in some undeveloped areas [2,3]. Hence, it is necessary and important to treat these Cr(VI)-containing wastewater.

Different methods have been employed for Cr(VI) removal from water bodies, such as redox processes [4], precipitation [5], electrocoagulation [6] and adsorption [7,8]. Among these methods, the adsorption has been widely used to remove heavy metals from aqueous environments due to its simplicity, reliability and safety and thus, could be a promising alternative for the removal of Cr(VI). Various adsorbents such as lignocellulose [9], activated carbon [10], chitosan [11], starch [12] and natural minerals [13]

---

*Corresponding author.

1944-3994/1944-3986 © 2014 Balaban Desalination Publications. All rights reserved.

have been employed to remove Cr(VI) from water bodies.

The mechanisms of Cr(VI) adsorption on materials mainly include van der Waals, covalent bonding and electrostatic interaction. To desorb Cr(VI) easily and reuse adsorbents, electrostatic interaction could be a promising alternative for the removal of Cr(VI) by adsorption and thus has received much consideration. Because Cr(VI) exists mainly in the form of anions in aqueous environments, the absorbent is expected to carry positive charge. Quaternary ammonium salt (QAS) is a type of organic compound that can ionise functional groups with positive charges and thus has attracted wide attention. Some researchers have used materials modified by QAS to remove anionic pollutants from aqueous environments [14,15]. Various supporting materials such as activated carbon [16], spent mushroom [17], cotton [18], bentonite [19], reed [20] and silica [21] have been reported. Among these supports, silica has high mechanical and thermal stability, which can be easily modified by organofunctionalised silanes through the formation of stable covalent bonds [22], and thus has been widely used. To increase the surface area of silica, it is usually prepared in its mesoporous form. In addition, magnetic materials such as magnetite (Fe_3O_4) and maghemite (γ-Fe_2O_3) have also been reported to be incorporated into silica, i.e. silica-encapsulated particles, to easily separate silica from aqueous environments after adsorption [23]. Few authors have reported the preparation of QAS-grafted magnetic materials and their application for the removal of pollutants [24–26]. However, most researchers used existing QAS, whereas *in situ* synthesis of QAS on the surface of silica is few.

In this study, a novel QAS with silane functional groups was designed and synthesised *in situ* on the surface of silica-encapsulated iron oxide nanoparticles (SEION) to be easily separated by an external magnet. Adsorption experiments were conducted to evaluate the capacity of the SEION grafted with QAS (QAS-SEION) for removing Cr(VI) from aqueous environments.

2. Materials and methods

2.1. Materials and chemicals

Tetraethoxysilane (TEOS) (99%), cetyltrimethylammonium bromide (CTAB) (99%), tetrahydrofuran (THF) (99%), 3-aminopropyltriethoxysilane (APTES) (99%), cyanuric chloride (99%), triethylamine (99.5%), toluene (99.5%), ammonia solution (25%), iron(II) sulphate heptahydrate (99%), iron(III) chloride anhydrous (99%), ethanol (95%) and potassium bichromate (99.8%) were purchased from Aldrich Chemical or Aladdin, Ltd. All of the chemicals were used without further treatment.

2.2. Synthesis of QAS

A 5.535 g of cyanuric chloride was dissolved in 100 mL of THF at 0℃. Then, 7 mL of APTES was added, and the solution was kept stirring at 0℃ for 3 h [27]. Subsequently, the temperature of this system was raised to 30℃, and 12.5 mL triethylamine was added; the solution was further kept stirring for 12 h. The products generated in the solution were collected and washed with THF three times and dried under vacuum at 60℃ for 12 h.

2.3. Synthesis of SEION

SEION was synthesised according to a procedure similar to that developed by Tsang [23]. A 7.289 g of CTAB was added to 125 mL of toluene under vigorous stirring to create a well-distributed suspension of CTAB in toluene. A 0.479 g of $FeSO_4{\cdot}7H_2O$ and 0.559 g of $FeCl_3$ were dissolved in 10 mL of deionised water. Then, the solution containing iron salts was added dropwise to the toluene suspension containing CTAB under an argon protective atmosphere to form a well-distributed microemulsion. The microemulsion was then stirred for at least 4 h. About 1.40 mL of ammonia solution (25% in water) was then added dropwise to the microemulsion under an argon protective atmosphere. The entire microemulsion immediately turned black, indicating the formation of magnetic Fe_3O_4. The chemical reaction is shown in Eq. (1).

$$\begin{aligned} &FeSO_4 + 2FeCl_3 + 8NH_3 \cdot H_2O \\ &\quad \longrightarrow Fe_3O_4 + (NH_4)_2SO_4 + 6NH_4Cl + 4H_2O \end{aligned} \tag{1}$$

After 2 h, 6.935 g of TEOS was slowly added to the microemulsion described above. The microemulsion was aged for 5 days at 25 ± 1℃ with constant stirring to allow the formation of a silica coating. Then, the stable and black microemulsion was destroyed by the addition of 20 mL of ethanol, and the black precipitates were separated using an external magnet. The residual TEOS and CTAB were then removed by refluxing the black precipitate with 200 mL of ethanol overnight and washing at least three times with ethanol and water, respectively. Finally, oxford grey precipitates, i.e. SEION product, were separated by an external magnet.

2.4. In situ *synthesis of QAS on SEION*

To a round flask containing 100 mL of toluene, 1 g of SEION and 5 mL of APTES were added under stirring to conduct a coupling process at 115˚C. After 12 h, the solids in the round flask were separated by an external magnet and washed with THF three times, and were then dispersed in 100 mL of THF. Subsequently, the temperature of this system was reduced to 0˚C by ice cooling prior to the addition of 4 g of cyanuric chloride. After 12 h, the solids in the round flask were separated again from THF by an external magnet to remove the unreacted reagents. Subsequently, 100 mL of THF was added, and the temperature of this system was raised to 30˚C, followed by the addition of 9 mL of triethylamine. After 12 h, the solids (i.e. QAS-SEION product) were again washed with THF and dried under vacuum at 60˚C for 12 h. The principal chemical reactions involved in QAS-SEION synthesis are illustrated in Fig. 1. The model structure and the magnetic response properties of the QAS-SEION are shown in Fig. 2. The saturation magnetisation of QM-chitosan is close to 13 emu/g which is sufficient to be used in adsorbent separation for further recycling and reuse.

2.5. *QAS-SEION characterisation*

Nuclear magnetic resonance (NMR) analysis of the QAS was carried out using an NMR spectrometer (Bruker Avance III 400 MHz). The surface charges of the QAS-SEION in solutions with different pH levels were determined using a zeta potential analyser (Zeta-Meter 3.0+). Scanning electron microscopy with energy dispersive X-ray spectroscopy (SEM/EDX, Hitachi S-3400N), transmission electron microscopy (TEM, Hitachi H-800), Fourier transform infrared spectrometry (FTIR, Nicolet AVATAR380) and X-ray diffraction (XRD, Bruker D2 Phaser) were employed to analyse the surface morphology, elemental components, surface functional groups and crystalline structures of the QAS-SEION, respectively.

2.6. *Batch experiments*

Experiments to investigate Cr(VI) removal by the QAS-SEION, including studies of the adsorption kinetics and isotherm and effects of adsorbent dosage, were conducted in 50-mL glass vials with screw caps containing Teflon-lined rubber septa. Briefly, 40 mL of Cr(VI) solutions and a certain amount of the QAS-SEION were mixed in 50-mL glass vials, and then shaken in an end-over-end manner at 26 rpm and 25 ± 1˚C. A 5 mM solution of NaCl was used as a background electrolyte to control the ionic strength of the solution. After a predefined reaction time, the solutions in the vials were rapidly filtered through 0.45-μm membranes, followed by immediate measurement of the Cr(VI) concentration by inductively coupled plasma optical emission spectroscopy (ICP-OES, Varian 700-ES) at a wavelength of 267.716 nm.

Desorption experiments of QAS-SEION were conducted using 50-mL glass vials. The QAS-SEION was firstly adsorbed to saturation by the high concentration Cr(VI) solution. Then, the QAS-SEION with

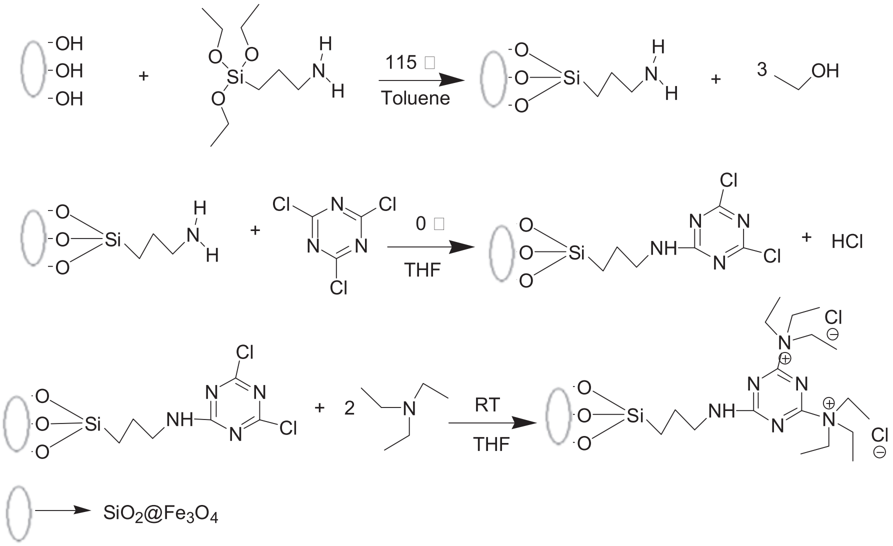

Fig. 1. *In situ* synthesis of QAS on SEION.

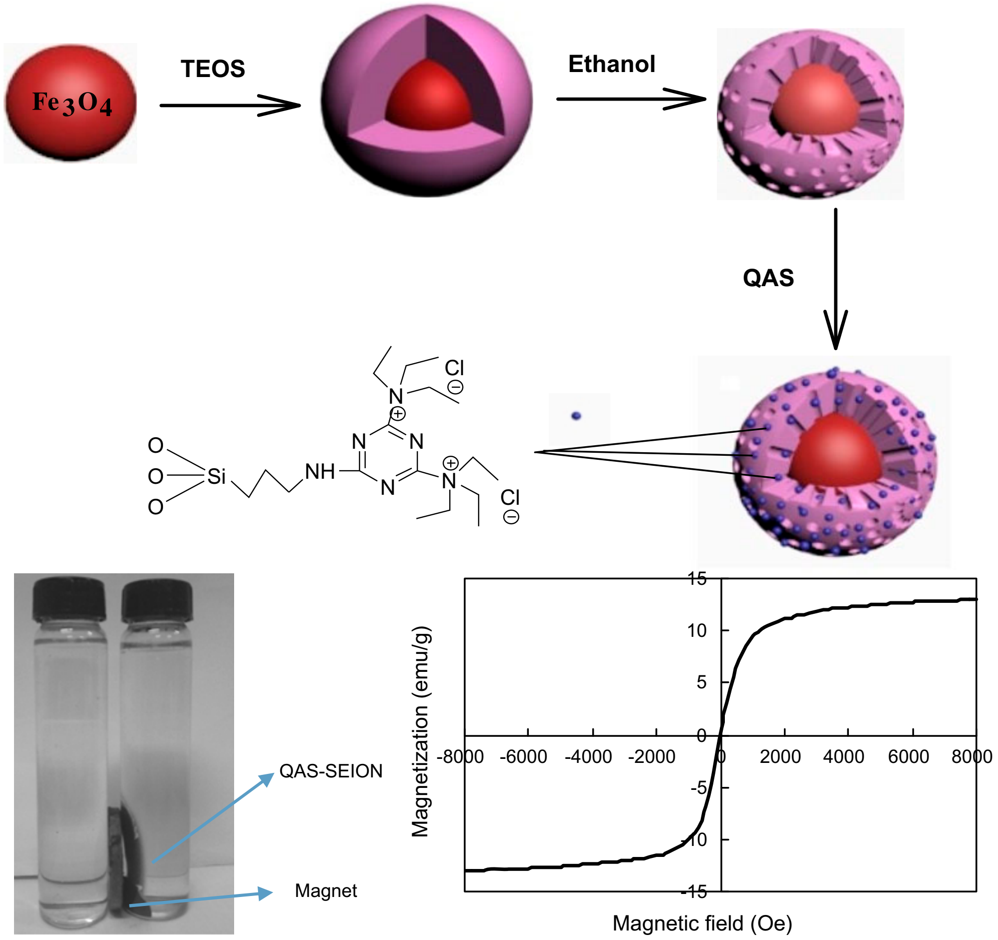

Fig. 2. Formation process and magnetic response properties of QAS-SEION.

the Cr(VI) was separated by filtration and vaccum-dried at 80°C for 48 h. Afterwards, 0.01 g of dried QAS-SEION with Cr(VI) and 40 mL of 2 mol/L NaCl solution were mixed in 50-mL glass vials, followed by shaking in an end-over-end manner at 26 r/min and at 25 ± 1°C for 12 h (pre-experiments indicated that desorption would reach equilibrium within 12 h). The suspensions with QAS-SEION were filtered and the Cr(VI) concentration was measured. The QAS-SEION on the filter was washed three times using deionised water and then vaccum-dried at 80°C for reuse.

3. Results and discussion

3.1. Characterisation of QAS and QAS-SEION

Fig. 3 shows the ^1H NMR ($CDCl_3$) spectrum of QAS. The chemical shifts near 1.33 ppm (CH_3) and 3.0 ppm (CH_2) were assigned to the ethyl bonded to N. The chemical shifts near 1.1 ppm (CH_3) and 3.9 ppm

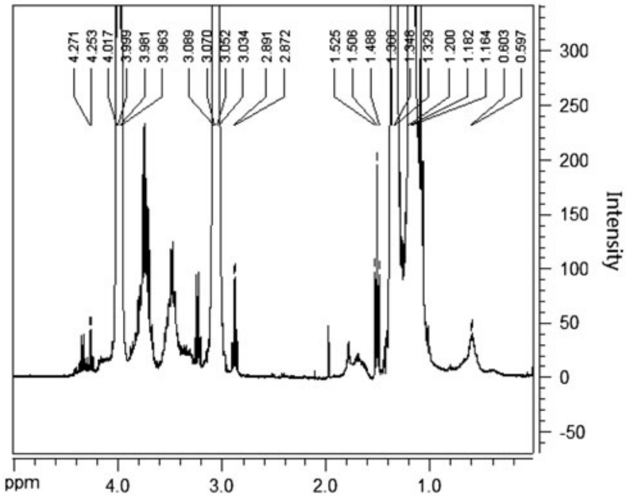

Fig. 3. ^1H NMR spectrum of QAS.

(CH_2) were assigned to the ethyl bonded to O. The chemical shift near 4.2 ppm was assigned to NH. Chemical shifts near 2.8 ppm, 1.4 ppm and 0.59 ppm were assigned to CH_2 between Si and N. Besides, the H integral areas are calculated. The results show that the ratios of integral areas of H chemical shifts at about 4.2, 3.9, 3.0, 2.8, 1.4, 1.33, 1.1 and 0.59 were 1:6.83:10.89:1.96:1.81:16.96:9.33:1.90, which was similar to theory ratio (1:6:12:2:2:18:9:2). The H chemical shifts and integral areas above indicated that the QAS was successfully synthesised.

Fig. 4 shows the XRD patterns of iron oxide (Fig. 4(a)) and the synthesised SEION (Fig. 4(b)). As shown in Fig. 4(a), seven typical peaks ($2\theta = 19.3^\circ$, 30.1°, 35.5°, 43.1°, 53.4°, 57.0° and 62.6°) were observed, which corresponded with the characteristic peaks of Fe_3O_4 ((1 1 1), (2 2 0), (3 1 1), (4 0 0), (4 2 2), (5 1 1) and (4 4 0)) [28]. Most of these peaks were also found in the SEION (Fig. 4(b)). Besides, a broad peak between 20° and 25° occurred in XRD pattern of SEION compared to Fe_3O_4, which covered the characteristic peak ($2\theta = 19.3^\circ$) of Fe_3O_4 and indicated that the silica covered on the Fe_3O_4 tended to be noncrystalline.

Fig. 5 shows the FTIR spectra of QAS, SEION and QAS-SEION. A broad peak at 3,300–3,600 cm^{-1} was observed for all samples, which was assigned to the stretching vibration of H_2O and indicated that a small amount of water existed in the samples [29]. For the QAS, the peaks at 1,500–1,700 cm^{-1} corresponded to C–N stretching vibration and aromatic ring vibration [30]. The peaks at 2,500–3,000 cm^{-1} were assigned to the stretching vibration of CH_3 and CH_2, which was echoed by the peaks at 1,200–1,500 cm^{-1} assigned to the bending vibration of CH_3 and CH_2 [31]. The peaks at 950–1,200 cm^{-1} were assigned to the Si–O stretching vibration and Si–C vibration of the QAS [30]. For the SEION, the peaks at 1,000–1,300 cm^{-1}, 700–800 cm^{-1} and 940–980 cm^{-1} were ascribed to the stretching vibrations of Si–O–Si, Si–OH and Si–O–Fe [32], respectively. Compared to the SEION spectrum, the peaks of the QAS-SEION at 1,500–1,700 cm^{-1} broadened, resulting from C–N stretching vibration and aromatic ring vibration of QAS grafted. In addition, the peaks at 940–980 cm^{-1} for the SEION did not occur in the spectrum of QAS-SEION, possibly due to the overlapping of Si–C vibration peak at 950–1,200 cm^{-1} with Si–O–Fe stretching vibration peak at 940–980 cm^{-1}. The occurrence of Si–C, C–N and aromatic ring vibration peaks for the QAS-SEION indicated that the QAS was successfully grafted on the SEION.

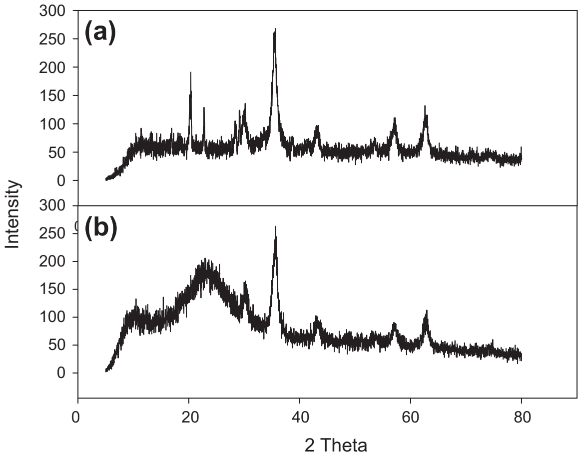

Fig. 4. XRD patterns of Fe_3O_4 (a) and SEION (b).

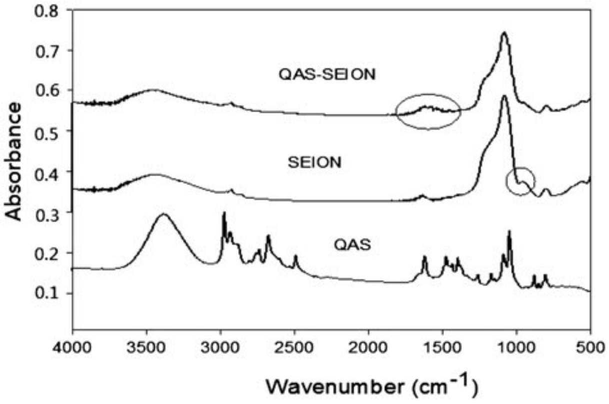

Fig. 5. FTIR spectra of QAS, SEION, and QAS-SEION.

TEM images and the SEM/EDX analysis results of the SEION and the QAS-SEION are shown in Figs. 6 and 7, respectively. Black particles, i.e. Fe_3O_4, were observed to disperse in the SEION (Fig. 6(a)) and the QAS-SEION (Fig. 6(b)), which can impart magnetic behaviour and facilitate their separation from the aqueous phase. The porous structure can be clearly observed in Fig. 6(a), which indicates that the SEION exhibit a larger specific surface area. However, the transparency of the pores shown in Fig. 6(b) decreased slightly, possibly resulting from grafting of the QAS on the SEION. SEM/EDX analysis revealed that Fe, Si and O were the major elements in the SEION (Fig. 7(a)). A small amount of C was also observed in the SEION, which may result from residual CTAB. Compared to the SEION composition, another element, Cl, was observed in the QAS-SEION (Fig. 7(b)), which was considered to be the counter ion of quaternary ammonium from the QAS and indicated that the QAS was successfully grafted onto the SEION. This inference was validated by zeta potentials of the SEION and the QAS-SEION. As shown in Fig. 8, the

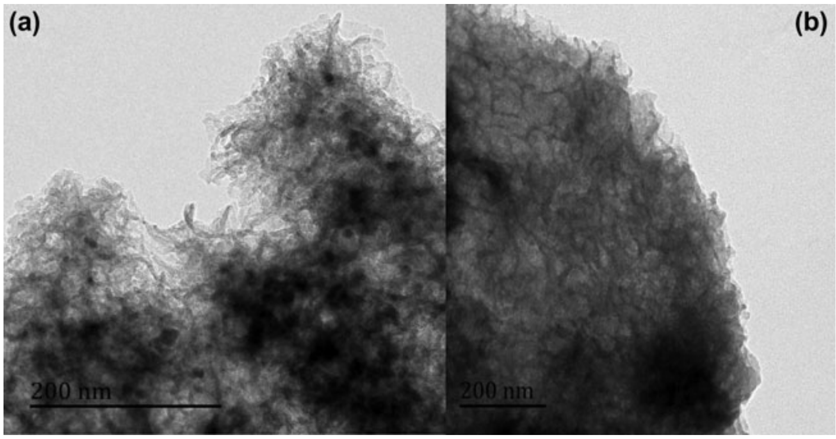

Fig. 6. TEM images of SEION (a) and QAS-SEION (b).

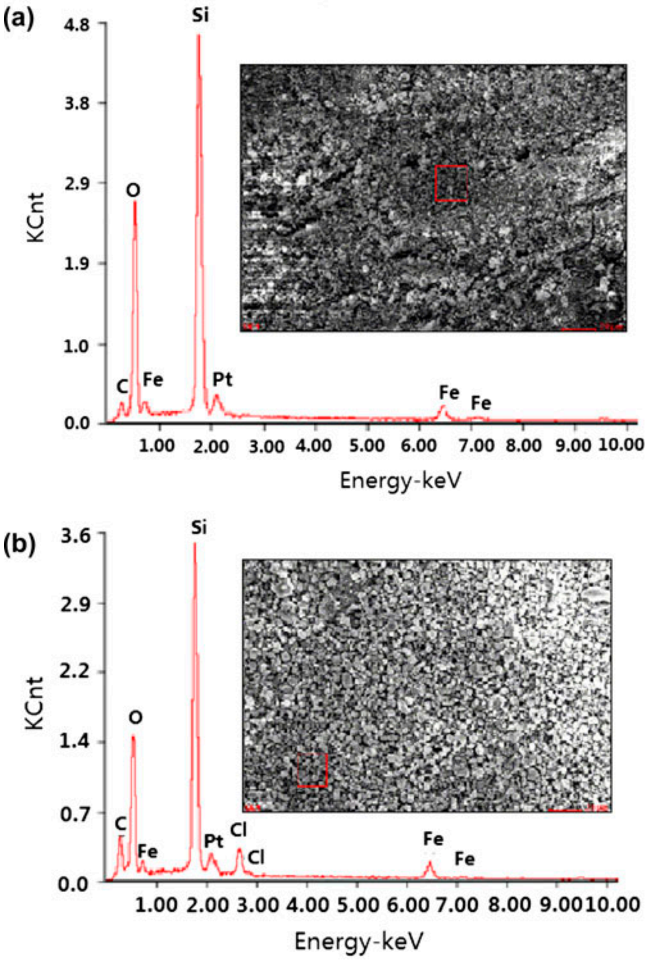

Fig. 7. SEM/EDX spectra of SEION (a) and QAS-SEION (b).

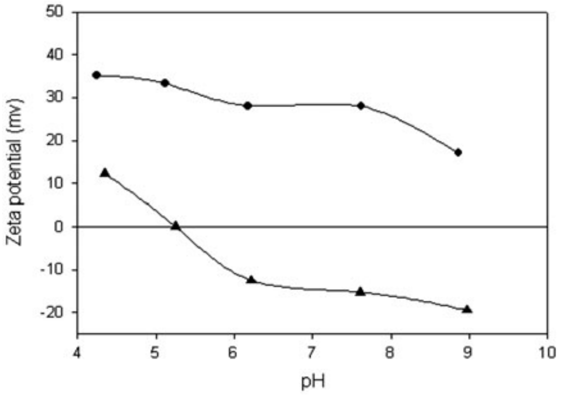

Fig. 8. Zeta potential of SEION (-▲-) and QAS-SEION (-●-) at different pH.

zeta potential of the SEION was negative except for at lower pH environment. However, the zeta potential of the QAS-SEION remained positive throughout the pH range investigated, which was significantly higher than the zeta potential of the SEION. The higher zeta potential of QAS-SEION mainly resulted from the QAS grafted on the SEION. As a consequence, anions and compounds with negative charges (e.g. CrO_4^{2-}, humic acid) can be easily adsorbed onto the QAS-SEION via electrostatic interaction.

3.2. *Adsorption of Cr(VI) on the QAS-SEION*

The kinetics of Cr(VI) removal by the QAS-SEION (Fig. 9) showed that the adsorption of Cr(VI) reached equilibrium within 120 min. The removal of Cr(VI) by the QAS-SEION may involve two main steps: Cr(VI) diffusion in the pores of the QAS-SEION and adsorption of Cr(VI) on the QAS-SEION. When the QAS-SEION is mixed with Cr(VI) solutions, Cr(VI) first diffuses into the QAS-SEION pores, depending on the concentration gradient, which takes time to

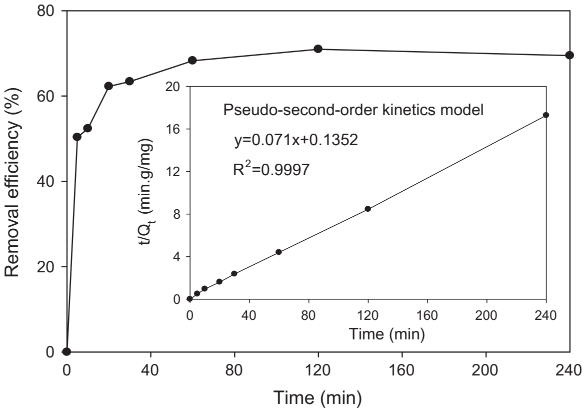

Fig. 9. Adsorption kinetics of Cr(VI) on QAS-SEION. The initial concentration of Cr(VI), 7.5 mg/L; QAS-SEION dosage, 0.01 g/40 mL and pH of the solution, 6.0 ± 0.1.

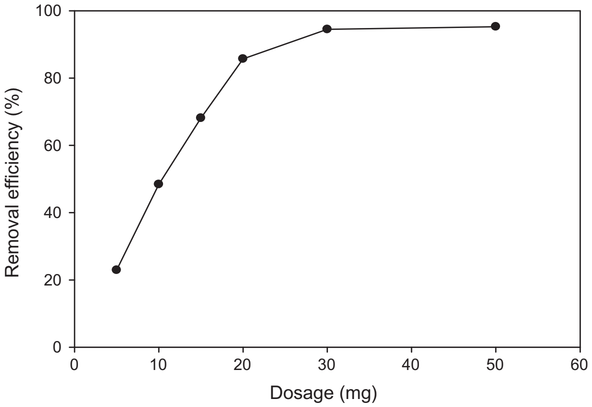

Fig. 10. Effects of QAS-SEION dosages on removal of Cr(VI). The initial concentration of Cr(VI), 10 mg/L; pH of the solution, 6.0 ± 0.1.

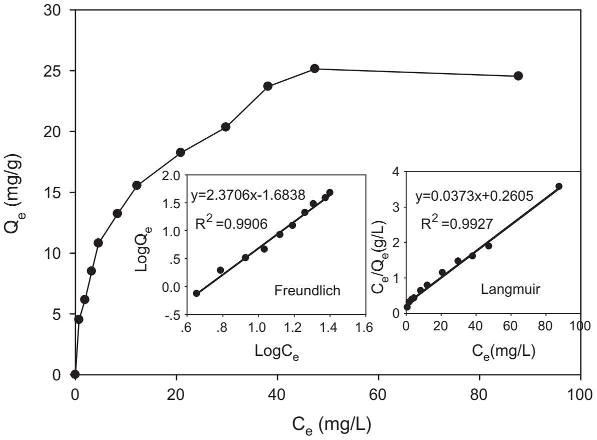

Fig. 11. Adsorption isotherm of Cr(VI) on QAS-SEION. QAS-SEION dosage, 0.01 g/40 mL; pH of the solution, 6.0 ± 0.1.

reach completion. Cr(VI) is then adsorbed on the QAS-SEION, where counter ions, i.e. chloride ions, are exchanged with Cr(VI), which is driven by electrostatic attraction. Among all of the steps of the entire adsorption process, the first step could be the rate-limiting step for Cr(VI) adsorption.

The kinetics of Cr(VI) adsorption on the QAS-SEION was fitted with a pseudo-second-order model [33] (Eq. 2).

$$\frac{t}{Q_t} = \frac{t}{kQ_e^2} + \frac{t}{Q_e} \tag{2}$$

The parameter k is the pseudo-second-order rate constant (g/(mg.min)), and Q_t and Q_e are the amounts of Cr(VI) adsorbed per unit mass (mg/g) at any time and at equilibrium, respectively.

The experimental results show that the kinetics of Cr(VI) adsorption on the QAS-SEION fit the pseudo-second-order model well with a reaction rate constant (k) of 0.0373 and a coefficient of determination (R^2) of 0.9997.

Fig. 10 shows the effect of QAS-SEION dosage on the removal of Cr(VI). As shown, the removal efficiency of Cr(VI) can reach 90% with a dosage of 30 mg of QAS-SEION in 40 mL of 7.5 mg/L Cr(VI) solution, whereas a dosage of 50 mg of QAS-SEION can achieve nearly 100% removal of Cr(VI). The study on the adsorbent dosage has practical importance for the application of the adsorbent.

To determine the largest amount of Cr(VI) adsorbed by the QAS-SEION, an isothermal adsorption experiment was conducted, and the adsorption isotherm is shown in Fig. 11. With the increase in the equilibrium concentration, the adsorption amount of Cr(VI) was observed to increase sharply at lower equilibrium concentrations, indicating a stronger affinity of Cr(VI) with the QAS-SEION. When the equilibrium concentration of Cr(VI) was close to 50 mg/L, the adsorption amount of Cr(VI) achieved the maximum.

In adsorption studies, different adsorption isotherm models (e.g. Langmuir model and Freundlich model) are usually used to simulate adsorption processes [34]. The Langmuir model assumes that all of the adsorption sites of the adsorbent have an identical binding energy and each site only binds to a single adsorbate, which is expressed as follows:

$$\frac{C_e}{Q_e} = \frac{1}{bQ_m} + \frac{C_e}{Q_m} \tag{3}$$

where C_e is the equilibrium concentration of the adsorbate, Q_m is the maximum adsorption capacity of the adsorbent and b is a constant related to the adsorption energy.

The Freundlich model is an empirical equation based on reversible heterogeneous adsorption and is expressed as:

$$\log Q_e = \frac{1}{n}\log C_e + \log K_f \tag{4}$$

where K_f is a constant related to the adsorption capacity of the adsorbent and n is a constant related to the adsorption intensity.

The adsorption isotherm of Cr(VI) on the QAS-SEION was fitted with the two models described above. As shown in Fig. 11, the Freundlich model suitably fits the adsorption isotherm of Cr(VI) before Cr(VI) reached saturated adsorption, whereas the Langmuir model may be used to simulate the adsorption of Cr(VI) at all equilibrium concentrations studied.

Table 1 shows the values of the Langmuir and Freundlich constants. The largest adsorption amount (26.81 mg/g) of Cr(VI) calculated was close to the experimental value (25.14 mg/g) shown in Fig. 11, higher than that reported [35,36].

3.3. Desorption and regeneration

The reusability of adsorbents is of great importance as a cost-effective process in water treatment. For the environmental sustainability of an adsorbent, a high regeneration capacity would add much value in water treatment. In this study, NaCl solution was chosen as the regeneration agent. Pre-experiments showed that the desorption efficiency of Cr(VI) increased with the increase of NaCl concentration. However, a high NaCl concentration would obviously result in a higher cost. In view of the above, 2.0 mol/L of NaCl was selected to regenerate the QAS-SEION. Three cycles of adsorption–desorption studies were accordingly carried out. The results showed that the QAS-SEION still had a high regeneration capacity after three adsorption–desorption cycles, which can be seen in Fig. 12 and indicate that the QAS-SEION is a promising adsorbent.

Table 1
Langmuir and Freundlich constants for Cr(VI) adsorption on QAS-SEION

Langmuir constants			Freundlich constants		
b	q_m	R^2	n	k_f	R^2
102.92	26.81	0.9927	0.422	0.021	0.9906

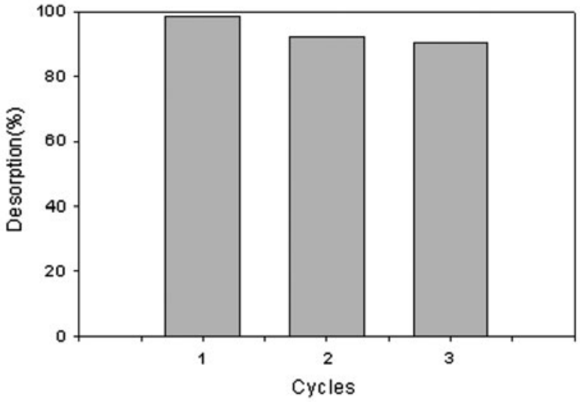

Fig. 12. Desorption of Cr(VI) from QAS-SEION.

4. Conclusions

In this study, a novel QAS was synthesised and successfully grafted onto SEION based on characteristic NMR, XRD, TEM, FTIR, SEM/EDX and zeta potential analyses. The new material, QAS-SEION, was used to remove Cr(VI) from aqueous environments. The QAS-SEION showed a strong magnetic response, which presents a great convenience in adsorbent separation for further recycling and reuse. The results of batch experiments demonstrated that the QAS-SEION can effectively remove Cr(VI) from aqueous environments. The adsorption kinetics were well-described by a pseudo-second-order equation. The adsorption isotherm fits both the Langmuir isotherm equation and Freundlich isotherm equation notably well. The maximum adsorption amount calculated by the Langmuir isotherm equation was close to that obtained by experiment. The adsorption–desorption of the QAS-SEION was evaluated, and high regeneration rates were demonstrated.

Acknowledgement

This work is supported by Innovation Projects from Shanghai Municipal Education Committee, China (12YZ153) and the State Key Laboratory of Pollution Control and Resource Reuse Foundation (PCRRF12019).

References

[1] G. Wójcik, V. Neagu, I. Bunia, Sorption studies of chromium(VI) onto new ion exchanger with tertiary amine, quaternary ammonium and ketone groups, J. Hazard. Mater. 190 (2011) 544–552.
[2] X. Li, J. Cao, W. Zhang, Stoichiometry of Cr(VI) immobilization using nanoscale zerovalent iron (nZVI): A

study with high-resolution X-ray photoelectron spectroscopy (HR-XPS), Ind. Eng. Chem. Res. 47 (2008) 2131–2139.

[3] P. Yuan, D. Liu, M. Fan, D. Yang, R. Zhu, F. Ge, J.X. Zhu, H. He, Removal of hexavalent chromium [Cr(VI)] from aqueous solutions by the diatomite-supported/unsupported magnetite nanoparticles, J. Hazard. Mater. 173 (2010) 614–621.

[4] E.L. Brodie, D.C. Joyner, B. Faybishenko, M.E. Conrad, C. Rios-Velazquez, J. Malave, R. Martinez, B. Mork, A. Willett, S. Koenigsberg, Microbial community response to addition of polylactate compounds to stimulate hexavalent chromium reduction in groundwater, Chemosphere 85 (2011) 660–665.

[5] A.K. Golder, A.K. Chanda, A.N. Samanta, S. Ray, Removal of hexavalent chromium by electrochemical reduction–precipitation: Investigation of process performance and reaction stoichiometry, Sep. Purif. Technol. 76 (2011) 345–350.

[6] Y. Ait Ouaissa, M. Chabani, A. Amrane, A. Bensmaili, Removal of Cr(VI) from model solutions by a combined electrocoagulation sorption process, Chem. Eng. Technol. 36 (2013) 147–155.

[7] I. Marzouk, C. Hannachi, L. Dammak, B. Hamrouni, Removal of chromium by adsorption on activated alumina, Desalin. Water Treat. 26 (2011) 279–286.

[8] G. Bayramoglu, M. Yakuparica, Adsorption of Cr(VI) onto PEI immobilized acrylate-based magnetic beads: Isotherms, kinetics and thermodynamics study, Chem. Eng. J. 139 (2008) 20–28.

[9] D.W. O'Connell, C. Birkinshaw, T.F. O'Dwyer, Heavy metal adsorbents prepared from the modification of cellulose: A review, Bioresour. Technol. 99 (2008) 6709–6724.

[10] P. Wang, R. Zhang, C. Hua, Removal of chromium (VI) from aqueous solutions using activated carbon prepared from crofton weed, Desalin. Water Treat. 51 (2013) 2327–2335.

[11] R. Huang, B. Yang, B. Wang, D. Zheng, Z. Zhang, Removal of chromium (VI) ions from aqueous solutions by N-2-hydroxypropyl trimethyl ammonium chloride chitosan–bentonite, Desalin. Water Treat. 50 (2012) 329–337.

[12] A. Dong, J. Xie, W. Wang, L. Yu, Q. Liu, Y. Yin, A novel method for amino starch preparation and its adsorption for Cu(II) and Cr(VI), J. Hazard. Mater. 181 (2010) 448–454.

[13] Y. Zhao, S. Yang, D. Ding, J. Chen, Y. Yang, Z. Lei, C. Feng, Z. Zhang, Effective adsorption of Cr(VI) from aqueous solution using natural Akadama clay, J. Colloid Interface Sci. 395 (2013) 198–204.

[14] J. Wu, L.M. Wang, P. Zhao, F. Wang, G. Wang, A new type of quaternary ammonium salt containing siloxane group and used as favorable dispersant in the surface treatment of C.I. Pigment red 170, Progr. Org. Coat. 63 (2008) 189–194.

[15] P.H. Rao, I.M.C. Lo, K. Yin, S.C.N. Tang, Removal of natural organic matter by cationic hydrogel with magnetic properties, J. Environ. Manage. 92 (2011) 1690–1695.

[16] J.H. Xu, N.Y. Gao, Y. Deng, M.H. Sui, Y.L. Tang, Perchlorate removal by granular activated carbon coated with cetyltrimethyl ammonium chloride, Desalination 275 (2011) 87–92.

[17] X. Jing, Y. Cao, X. Zhang, D. Wang, X. Wu, H. Xu, Biosorption of Cr(VI) from simulated wastewater using a cationic surfactant modified spent mushroom, Desalination 269 (2011) 120–127.

[18] S. Deng, Y.Q. Zheng, F.J. Xu, B. Wang, J. Huang, G. Yu, Highly efficient sorption of perfluorooctane sulfonate and perfluorooctanoate on a quaternized cotton prepared by atom transfer radical polymerization, Chem. Eng. J. 193–194 (2012) 154–160.

[19] T. Kan, X. Jiang, L. Zhou, M. Yang, M. Duan, P. Liu, X. Jiang, Removal of methyl orange from aqueous solutions using a bentonite modified with a new gemini surfactant, Appl. Clay Sci. 54 (2011) 184–187.

[20] S. Baidas, B.Y. Gao, X.G. Meng, Perchlorate removal by quaternary amine modified reed, J. Hazard. Mater. 189 (2011) 54–61.

[21] P. Wang, Q. Shi, Y. Shi, K.K. Clark, G.D. Stucky, A.A. Keller, Magnetic permanently confined micelle arrays for treating hydrophobic organic compound contamination, J. Am. Chem. Soc. 131 (2009) 182–188.

[22] G. Grigoropoulou, P. Stathi, M.A. Karakassides, M. Louloudi, Y. Deligiannakis, Functionalized SiO_2 with N-, S-containing ligands for Pb(II) and Cd(II) adsorption, Colloids Surf., A 320 (2008) 25–35.

[23] S.C. Tsang, C.H. Yu, X. Gao, K. Tam, Silica-encapsulated nanomagnetic particle as a new recoverable biocatalyst carrier, J. Phys. Chem. B 110 (2006) 16914–16922.

[24] J. Liu, X. Du, Fast removal of aqueous Hg(II) with quaternary ammonium-functionalized magnetic mesoporous silica and silica regeneration, J. Mater. Chem. 21 (2011) 6981–6987.

[25] H.T. Wang, A.A. Keller, K.K. Clark, Natural organic matter removal by adsorption onto magnetic permanently confined micelle arrays, J. Hazard. Mater. 194 (2011) 156–161.

[26] K.Z. Elwakeel, Removal of Cr(VI) from alkaline aqueous solutions using chemically modified magnetic chitosan resins, Desalination 250 (2010) 105–112.

[27] I.I. Ebralidze, M. Hanif, R. Arjumand, A.A. Azmi, D. Dixon, N.M. Cann, C.M. Crudden, J.H. Horton, Solvent induced adhesion interactions between dichlorotriazine films, J. Phys. Chem. C 116 (2012) 4217–4223.

[28] R. Rahimi, A. Maleki, S. Maleki, A. Morsali, M.J. Rahimi, Synthesis and characterization of magnetic dichromate hybrid nanomaterials with triphenylphosphine surface modified iron oxide nanoparticles ($Fe_3O_4@SiO_2@PPh_3@Cr_2O_7^{2-}$), Solid State Sciences 28 (2014) 9–13.

[29] Z.Y. Lin, Y.X. Zhang, Y.L. Chen, H. Qian, Extraction and recycling utilization of metal ions (Cu^{2+}, Co^{2+} and Ni^{2+}) with magnetic polymer beads, Chem. Eng. J. 200–202 (2012) 104–112.

[30] F. Adam, K.M. Hello, H. Osman, The heterogenation of melamine and its catalytic activity, Appl. Catal. A 382 (2010) 115–121.

[31] P. Wu, J. Zhu, Z. Xu, Template-assisted synthesis of mesoporous magnetic nanocomposite particles, Adv. Funct. Mater. 14 (2004) 345–351.

[32] P.I. Girginova, A.L. Daniel-da-Silva, C.B. Lopes, P. Figueira, M. Otero, V.S. Amaral, E. Pereira, T. Trindade, Silica coated magnetite particles for magnetic removal of Hg^{2+} from water, J. Colloid Interface Sci. 345 (2010) 234–240.

[33] J. Zhang, S. Zhai, S. Li, Z. Xiao, Y. Song, Q. An, G. Tian, Pb(II) removal of Fe_3O_4@SiO_2-NH_2 core–shell nanomaterials prepared via a controllable sol–gel process, Chem. Eng. J. 215–216 (2013) 461–471.

[34] Y.A. Aydın, N.D. Aksoy, Adsorption of chromium on chitosan: Optimization, kinetics and thermodynamics, Chem. Eng. J. 151 (2009) 188–194.

[35] L. Panda, B. Das, D.S. Rao, B.K. Mishra, Application of dolochar in the removal of cadmium and hexavalent chromium ions from aqueous solutions, J. Hazard. Mater. 192 (2011) 822–831.

[36] Z. Sadaoui, S. Hemidouche, O. Allalou, Removal of hexavalent chromium from aqueous solutions by micellar compounds, Desalination 249 (2009) 768–773.